

QCD saturation and $\gamma^*-\gamma^*$ scattering

M. Kozlov^{1,a}, E. Levin^{1,2,b}

¹ HEP Department, School of Physics and Astronomy, Raymond and Beverly Sackler Faculty of Exact Science,
 Tel Aviv University, Tel Aviv, 69978, Israel

² DESY Theory Group, 22603, Hamburg, Germany

Received: 22 November 2002 / Revised version: 27 January 2003 /
 Published online: 5 May 2003 – © Springer-Verlag / Società Italiana di Fisica 2003

Abstract. Two photon collisions at high energy have an important theoretical advantage: the simplicity of the initial state, which gives us a unique opportunity to calculate these processes for large virtualities of both photons in the perturbative QCD approach. In this paper we study QCD saturation in two photon collisions in the framework of the Glauber–Mueller approach. The Glauber–Mueller formula is derived emphasising the impact parameter dependence (b_t) of the dipole–dipole amplitude. It is shown that non-perturbative QCD contributions are needed to describe the large b_t behaviour, and the way how to deal with them is suggested. Our approach can be viewed as the model for the saturation in which the entire impact parameter dependence is determined by the initial conditions. The unitarity bound for the total cross section, its energy dependence as well as predictions for future experiments are discussed. It is argued that the total cross section increases faster than any power of $\ln(1/x)$ in a wide range of energy or x , namely $\sigma(\gamma^*-\gamma^*) \propto (1/Q^2) \exp(a\sqrt{\ln(1/x)}) \leq 1/m_\pi^2$, where $\exp(a\sqrt{\ln(1/x)})$ reflects the x dependence of the gluon density $xG \propto \exp(2a\sqrt{\ln(1/x)})$ and m_π is the pion mass.

1 Introduction

Two photon collisions at high energy have three theoretical advantages over hadronic collisions and/or deep inelastic scattering.

(1) The simplicity of the initial state, which allows processes, such as large transverse momentum hadronic jet production, to be calculated exactly to lowest order in perturbative theory. With the advent of high quality experimental data, theoretical analyses also focus on higher order corrections to the basic processes which can provide an interesting test of the theory [1].

(2) Scattering of two photons with large but equal virtualities gives unique access to BFKL emission [2], making this process very useful for studying the dynamics [3–9].

(3) Scattering of two virtual photons with large virtualities allows one to study shadowing (screening) corrections on the solid theoretical basis of perturbative QCD [10].

It is well known that the correct degrees of freedom at high energy are not quarks or gluons but colour dipoles [11–14] which have transverse sizes r_t and a fraction of energy x . Therefore, two photon interactions occur in two successive steps. First, each of the virtual photons decays into a colour dipole (quark–antiquark pair) with size r_t . At large values of the virtualities the probability of such a

decay can be calculated in pQCD. The second stage is the interaction of colour dipoles with each other. The simple formula (see for example [15]) that describes the process of the interaction of two photons with virtualities Q_1 and Q_2 is (see Fig. 1)

$$\begin{aligned} \sigma(Q_1, Q_2, W) &= \int d^2b_t \sum_{a,b}^{N_f} \int_0^1 dz_1 \int d^2dr_{1,t} |\Psi_{T,L}^a(Q_1; z_1, r_{1,t})|^2 \\ &\times \int_0^1 dz_2 \int d^2dr_{2,t} |\Psi_{T,L}^b(Q_2; z_2, r_{2,t})|^2 \\ &\times \sigma_{a,b}^{dd}(\tilde{x}_{ab}, r_{1,t}, r_{2,t}; b_t), \end{aligned} \quad (1.1)$$

where the indices a and b specify the flavours of the interacting quarks, and T and L indicate the polarization of the interacting photons. The r_i denote the transverse separation between quark and antiquark in the dipole (dipole size) and z_i are the energy fractions of the quark in the photon i . $\sigma_{ab}^{dd} = 2N((\tilde{x}_{ab}, r_{1,t}, r_{2,t}; b_t)$, where N is the imaginary part of the dipole–dipole amplitude at energy x given by

$$\tilde{x}_{ab} = \frac{Q_1^2 + Q_2^2 + 4m_a^2 + 4m_b^2}{W^2 + Q_1^2 + Q_2^2}, \quad (1.2)$$

where m_a is the mass of the quark with flavour a . b_t is the impact parameter for the dipole–dipole interaction and

^a e-mail: kozlov@post.tau.ac.il

^b e-mail: leving@post.tau.ac.il and levin@mail.desy.de

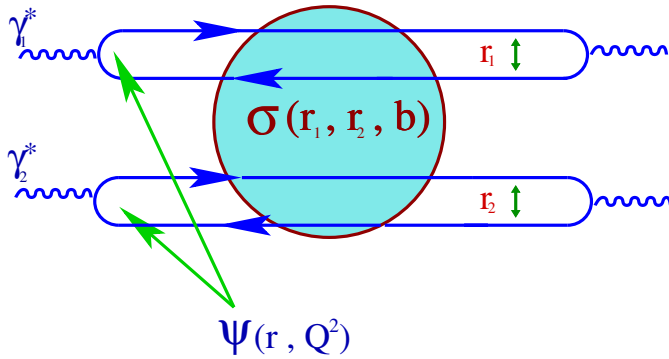


Fig. 1. The picture of the interaction of two photons with virtualities Q_1 and Q_2 larger than a “soft” scale

it is equal to the transverse distance between the dipole centers of mass. It is clear that σ_{ab}^{dd} has the meaning of $d\sigma/d^2b_t$.

The wave functions for virtual photons are known [16]; they are given by

$$|\Psi_T^a(Q; z, r_t)|^2 = \frac{6\alpha_{em}}{\pi^2} Z_a^2 ((z^2 + (1-z)^2) \bar{Q}_a^2 K_1^2(\bar{Q}_a r_t) + m_a^2 K_0^2(\bar{Q}_a r_t)) \quad (1.3)$$

$$|\Psi_L^a(Q; z, r_t)|^2 = \frac{6\alpha_{em}}{\pi^2} Z_a^2 Q^2 z^2 (1-z)^2 K_0^2(\bar{Q}_a r_t), \quad (1.4)$$

with $\bar{Q}_a^2 = z(1-z)Q^2 + m_a^2$, where Z_a and m_a denote the fraction of charge and mass of the quark of flavour a .

The main contribution in (1.1) is concentrated at $r_{1,t} \approx 1/Q_1 \ll 1/\mu$ and $r_{2,t} \approx 1/Q_2 \ll 1/\mu$, where μ is the soft mass scale. Therefore, at first sight, we can safely use pQCD for the calculation of the dipole–dipole cross section σ in (1.1). The objective of this paper is to investigate the dipole–dipole cross section at high energy (low x) where QCD saturation is expected [17–19]. The first analysis based on the Golec–Biernat and Wüsthoff model [20] has been performed in [10]. Here we will extend this analysis by using the Glauber–Mueller approach [11–13] with special focus on the impact parameter dependence which was completely omitted in the GBW model as well as in [10].

In the next section we discuss the dipole–dipole interaction in the Born approximation of pQCD. We show that this approximation leads to σ which decreases as a power of b_t . It turns out that $\sigma \rightarrow 1/b_t^4$ for large $b_t > r_{1,t}$ and $r_{2,t}$. Of course, such a behaviour will not change its character in higher orders of pQCD [21–24] since it is a direct consequence of the massless gluon in QCD. Using the Born approximation as an example we consider the non-perturbative contribution that provides an exponential decrease at large values of $b_t > 1/m_\pi$.

Section 3 is devoted to the Glauber–Mueller formula in the case of the DGLAP emission [25]. Here, we use the advantage of photon–photon scattering with large photon virtualities, since we can calculate the gluon density without uncertainties related to non-perturbative initial distributions in the hadronic target. It is well known that no b_t dependence is induced by DGLAP emission at least

for large values of the impact parameter. Therefore, the entire impact parameter dependence is due to the Born approximation cross section. In other words, we can use our approach as an explicit illustration of the point of view that the non-perturbative large $b_t \geq 1/2m_\pi$, where m_π is the pion mass, is determined by the initial condition [29,30] in contrast with the notion that such a behaviour could change the kernel of the non-linear equation that governs the evolution in the saturation region [21–24].

The unitarity bounds as well as the different regimes of the energy behaviour of two photon total cross sections are considered in Sect. 4.

In Sect. 5 we give our estimates for the values of the total cross sections for the accessible range of energy.

In the last section we summarize our results.

2 Dipole–dipole interaction in the Born approximation

The Born approximation for the dipole–dipole scattering amplitude is shown in Fig. 2.

To obtain the expression for $\sigma^{dd}(\tilde{x}, r_{1,t}, r_{2,t}; b_t)$ (see Fig. 1) we need to calculate the diagrams in the momentum representation and than to rewrite them in space-time representations. The conjugated variables to p_t and l_t will have the size of the dipole (say $r_{1,t}$ and the impact parameter b_t). The detailed calculation performed by the light-cone technique (see for example [26]) has been performed in [27]. The answer is

$$\sigma(\tilde{x}, r_{1,t}, r_{2,t}; b_t) = \pi\alpha_S^2 \frac{N_c^2 - 1}{2N_c^2} \times \left(\ln \frac{(\vec{b} - z_1\vec{r}_1 - z_2\vec{r}_2)^2 (\vec{b} - \bar{z}_1\vec{r}_1 - \bar{z}_2\vec{r}_2)^2}{(\vec{b} - \bar{z}_1\vec{r}_1 - z_2\vec{r}_2)^2 (\vec{b} - z_1\vec{r}_1 - \bar{z}_2\vec{r}_2)^2} \right)^2, \quad (2.5)$$

where z_i is the fraction of the energy of the dipole carried by the quarks and $\bar{z}_i = z_i - 1$. All vectors are two dimensional in (2.5).

Equation (2.5) has a simpler form if we assume that $z_i = 1/2$. Namely,

$$\sigma(\tilde{x}, r_{1,t}, r_{2,t}; b_t) = \pi\alpha_S^2 \frac{N_c^2 - 1}{2N_c^2} \times \left(\ln \frac{(\vec{b} + \vec{R})^2 (\vec{b} - \vec{R})^2}{(\vec{b} + \vec{\Sigma})^2 (\vec{b} - \vec{\Sigma})^2} \right)^2, \quad (2.6)$$

where $\vec{R} = \frac{\vec{r}_{1,t} - \vec{r}_{2,t}}{2}$ and $\vec{\Sigma} = \frac{\vec{r}_{1,t} + \vec{r}_{2,t}}{2}$. We note that we do not find the dipole–dipole cross section in the impact parameter representation in [27], but the calculation is so simple that we just present the answer.

To simplify our further calculations we restrict ourselves by DGLAP emission assuming that $r_{1,t}$ is much smaller than $r_{2,t}$. It is instructive to find two different limits in (2.5).

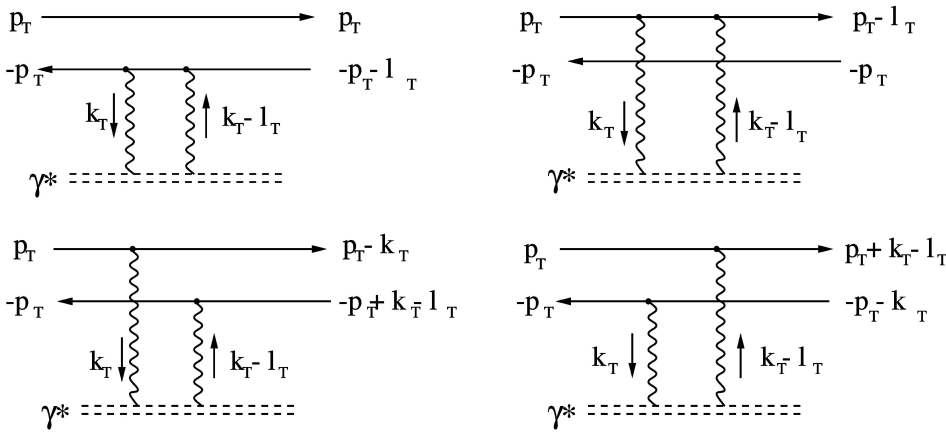


Fig. 2. The Born approximation for dipole-dipole scattering amplitude

(1) $b_t \gg r_{2,t} \gg r_{1,t}$. Expanding (2.5) one can obtain after integration over the azimuthal angle

$$\sigma(\tilde{x}, r_{1,t}, r_{2,t}; b_t) \rightarrow \pi \alpha_S^2 \frac{N_c^2 - 1}{N_c^2} \frac{r_{1,t}^2 r_{2,t}^2}{b_t^4}. \quad (2.7)$$

(2) $b_t \ll r_{1,t} \ll r_{2,t}$. We have

$$\sigma(\tilde{x}, r_{1,t}, r_{2,t}; b_t) \rightarrow \pi \alpha_S^2 \frac{N_c^2 - 1}{N_c^2} \frac{r_{1,t}^2 r_{2,t}^2}{z_2^2 \bar{z}_2^2 r_{2,t}^4}. \quad (2.8)$$

(3) Therefore, we can suggest a simple formula which covers two these limits, namely

$$\sigma(\tilde{x}, r_{1,t}, r_{2,t}; b_t) = \pi \alpha_S^2 \frac{N_c^2 - 1}{N_c^2} \frac{r_{1,t}^2 r_{2,t}^2}{(b_t^2 + z_2 \bar{z}_2 r_{2,t}^2)^2}. \quad (2.9)$$

For further estimates we will use (2.9) which reflects all qualitative features of the full expression of (2.5) but considerably simplifies the calculations.

Equation (2.5) as well as (2.9) leads to a power-like decrease at large values of b_t , namely, $\sigma(\tilde{x}, r_{1,t}, r_{2,t}; b_t) \propto 1/b_t^4$. Such a behaviour cannot be correct since it contradicts the general consequence of analyticity and crossing symmetry of the scattering amplitude. Since the spectrum of hadrons has no particles with mass zero, the scattering amplitude should decrease as $e^{-2m_\pi b_t}$ [28]. Certainly we need to take into account non-perturbative corrections to heal this problem, as has been noticed in many papers [29, 21–24, 30]. We suggest the procedure how to introduce such corrections which is based on the hadron-parton duality in the spirit of the QCD sum rules [31]. This procedure consists of two steps:

(i) first, we rewrite (2.9) in the momentum transfer representation ($t = -q_t^2$) in the form of a dispersion relation with respect to the mass of two gluons in the t -channel;

(ii) secondly, we claim that this dispersion integral gives the correct contribution of all hadronic states on average. Therefore, the model for the non-perturbative contribution is the integral over a two gluon state in the t -channel but with the restriction that the two gluon mass should be larger than the minimum mass in hadronic states, namely,

larger than $2m_\pi$. As in QCD sum rules [31] we assume that the integrand at large mass of the two gluon state can be found in perturbative QCD, while for small mass we have to include the realistic (experimental) spectrum of hadrons. The integration from $2m_\pi$ means that we believe that we can approximate the dispersion integral even in the region of small masses by the perturbative QCD contribution. This procedure corresponds to the approximation that has been used in [30]. We can also evaluate this integral differently: taking into account the first resonance (glueball) explicitly and to use the pQCD approach to estimate the dispersion integral for masses larger than s_0 , the value for s_0 can be taken from a QCD sum rules calculation of the glueball spectrum [31]. Such an approach is closely related to the one developed in [29], and it appears reasonable in pure gluodynamics where we do not have any pions.

Rewriting (2.9) in the form

$$\sigma(\tilde{x}, r_{1,t}, r_{2,t}; b_t) = \frac{C(r_{1,t}, r_{2,t})}{(b_t^2 + a^2)^2}, \quad (2.10)$$

with obvious notation, we can see that

$$\begin{aligned} \sigma(\tilde{x}, r_{1,t}, r_{2,t}; q^2) &= C(r_{1,t}, r_{2,t}) \int b_t db_t \frac{J_0(bq)}{(b_t^2 + a^2)^2} \\ &= C(r_{1,t}, r_{2,t}) \frac{q}{2a} K_1(aq), \end{aligned} \quad (2.11)$$

where J_0 and K_1 are Bessel and McDonald functions respectively. However, we can rewrite $K_1(aq)$ in a different way as

$$q K_1(aq) = \int \frac{J_1(\kappa a) \kappa^2 d\kappa}{\kappa^2 + q^2}. \quad (2.12)$$

The last integral, (2.12), gives the dispersion relation, namely,

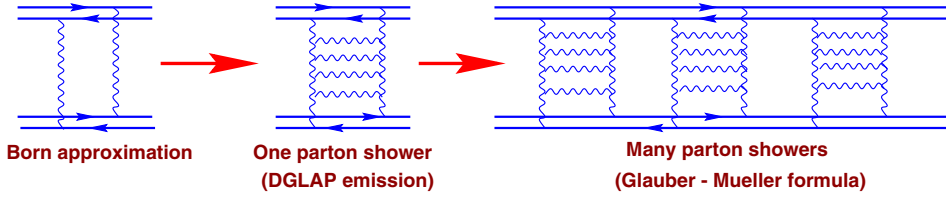


Fig. 3. The Glauber–Mueller approach for dipole–dipole scattering amplitude

$$\begin{aligned} \sigma(\tilde{x}, r_{1,t}, r_{2,t}; t = -q^2) \\ = C(r_{1,t}, r_{2,t}) \frac{1}{2a} \int_0^\infty \frac{J_1(\kappa a) \kappa^2 d\kappa}{\kappa^2 - t}; \end{aligned} \quad (2.13)$$

we replace (2.13) by

$$\begin{aligned} \sigma(\tilde{x}, r_{1,t}, r_{2,t}; t = -q^2) \\ = C(r_{1,t}, r_{2,t}) \frac{1}{2a} \int_{2m_\pi}^\infty \frac{J_1(\kappa a) \kappa^2 d\kappa}{\kappa^2 - t}, \end{aligned} \quad (2.14)$$

in accordance with our main idea. Returning to the impact parameter representation we obtain

$$\begin{aligned} \sigma(\tilde{x}, r_{1,t}, r_{2,t}; b_t) \\ = C(r_{1,t}, r_{2,t}) \frac{1}{2a} \int_{2m_\pi}^\infty \kappa^2 d\kappa \int_0^\infty q dq \frac{J_1(\kappa a) J_0(q b_t)}{\kappa^2 + q^2} \\ = \pi \alpha_S^2 \frac{N_c^2 - 1}{2N_c^2} r_{1,t}^2 r_{2,t}^2 \\ \times \frac{1}{\sqrt{z_2 \bar{z}_2} r_{2,t}} \int_{2m_\pi}^\infty \kappa^2 d\kappa J_1(\kappa a) K_0(\kappa b_t). \end{aligned} \quad (2.15)$$

One can see that $\sigma \propto e^{-2m_\pi b_t}$ for $b_t \gg 1/2m_\pi$ due to the asymptotic behaviour of the McDonald function $K_1(\kappa b_t) \rightarrow e^{-2m_\pi b_t}$ at large b_t .

Therefore, the b_t behaviour is: for $1/(2m_\pi) > b_t > r_{1,t}$ and/or $r_{2,t}$ the dipole–dipole scattering amplitude falls as $1/b_t^4$, but for large b_t ($b_t > 1/(2m_\pi)$) we have a normal exponential decrease: $e^{-2m_\pi b_t}$, which has a non-perturbative origin. Equation (2.15) gives us a rather general way to take into account the non-perturbative contribution, since in this equation we explicitly introduce the minimum mass in the experimental hadronic spectrum. However, as we have mentioned above, we can expect a large mass for the low limit of integration in the dispersion relation of (2.14) and (2.15) ($\tilde{Q}_0 > m_\pi$) which will lead to a $\sigma(\tilde{x}, r_{1,t}, r_{2,t}; b_t)$ behaviour $\propto e^{-\tilde{Q}_0 b_t}$.

3 Glauber–Mueller formula

The Glauber–Mueller approach takes into account the interaction of many parton showers with the target as it is shown in Fig. 3. Actually this formula was suggested in [13, 12] but Mueller [11] was the first who proved this formula especially for the gluon parton density. The main idea of this approach is that colour dipole is the correct degree of freedom for high energy scattering¹. Indeed, the

change of the value of the dipole size r_t (Δr_t) during the passage of the colour dipole through the target is proportional to the number of rescatterings (or the size of the target R) multiplied by the angle k_t/E where E is the energy of the dipole and k_t is the transverse momentum of the t -channel gluon which is emitted by the fast dipole. We have

$$\Delta r_t \propto R \frac{k_t}{E}. \quad (3.16)$$

Since k_t and r_t are conjugate variables and due to the uncertainty principle

$$k_t \propto \frac{1}{r_t}.$$

Therefore,

$$\Delta r_t \propto R \frac{k_t}{E} \ll r_t \text{ if } R \ll r_t^2 E \text{ or } x \ll \frac{1}{2mR}. \quad (3.17)$$

3.1 DGLAP emission

We first discuss the generalization of the Born approximation to include the DGLAP emission (see Fig. 3). This will give us the correct description of the one parton shower interaction. The DGLAP equation looks very simple in the region of low x , namely,

$$\begin{aligned} \frac{\partial^2 xG(x, r_{1,t}^2, r_{2,t}^2)}{\partial \ln(1/x) \partial \ln(1/r_{1,t}^2)} \\ = \frac{N_c}{\pi} \alpha_S(r_{1,t}^2) xG(x, r_{1,t}^2, r_{2,t}^2), \end{aligned} \quad (3.18)$$

where we consider $r_{1,t} \ll r_{2,t}$ and rewrite the DGLAP equation in coordinate space. We would like to recall that the DGLAP evolution equation sums the $(\alpha_S \log Q^2)^n$ contribution, and therefore, we can safely rewrite it in the coordinate representation, since within logarithmic accuracy $\ln Q^2 = \ln(1/r_t^2)$. The initial condition for (3.18) is $xG(x = x_0, r_{1,t}^2, r_{2,t}^2) = 1$. This means that the dipole–dipole cross section at fixed b_t for one parton shower interaction has the form (

$$\begin{aligned} \sigma_{\text{dipole}}(x, r_{1,t}, r_{2,t}; b_t) \\ = \sigma_{\text{dipole}}^{\text{BA}}(x, r_{1,t}, r_{2,t}; b_t) xG(x, r_{2,t}^2, r_{2,t}^2), \end{aligned} \quad (3.19)$$

where $\sigma_{\text{dipole}}^{\text{BA}}$ is the Born approximation for the dipole cross section.

The obvious solution is

$$xG(x, r_{1,t}^2, r_{2,t}^2) = I_0 \left(2\sqrt{\xi(r_{1,t}, r_{2,t}) \ln(1/x)} \right), \quad (3.20)$$

¹ This idea was formulated by Mueller in [14] a bit later.

where

$$\xi(r_{1,t}, r_{2,t}) = \frac{12 N_c}{11 N_c - 2 N_f} \ln \frac{\ln(4/(r_{1,t}^2 \Lambda^2))}{\ln(4/(r_{2,t}^2 \Lambda^2))}.$$

Here, in the arguments of the running QCD coupling we have made the simple replacement $Q^2 \rightarrow 4/r_t^2$. Within log accuracy we cannot guarantee the coefficient 4 in this expression but as was argued in [34] this is a reasonable choice (approximation).

Equation (3.20) has the following asymptotic behaviour:

$$xG(x, r_{1,t}^2, r_{2,t}^2) \rightarrow e^{2\sqrt{\xi(r_{1,t}, r_{2,t}) \ln(1/x)}}, \quad (3.21)$$

which means that xG grows faster than any power of $\ln(1/x)$.

Strictly speaking (3.18) is proven in the so-called double log approximation of perturbative QCD, in which we consider

$$\begin{aligned} \alpha_S \ln(1/x) \ln(Q_1^2/Q_2^2) &\approx 1; \\ \alpha_S \ln(1/x) &< 1; \\ \alpha_S \ln(Q_1^2/Q_2^2) &< 1; \\ \alpha_S &\ll 1. \end{aligned} \quad (3.22)$$

However, we will use this equation in a wider kinematic region where $\alpha_S \ln(1/x) \ln(Q_1^2/Q_2^2) > 1$ and $\alpha_S \ln(1/x) > 1$, while $\alpha_S \ln(Q_1^2/Q_2^2) \approx 1$. In this kinematic region we should use the BFKL equation [2]. We view (3.18) as the limit of the BFKL equation in which we take into account the logarithmic contribution in the transverse momentum integration in the BFKL kernel. The justification for such an approach is the fact that the anomalous dimension of the DGLAP equation can be parameterized in a simple way [32]:

$$\gamma(\omega) = \alpha_S \left(\frac{1}{\omega} - 1 \right) \quad (3.23)$$

The first term in (3.23) leads to (3.18) in the region of low x .

Equations (3.19) and (3.20) solve the problem of one parton shower interaction in the DGLAP evolution. It should be stressed that the impact parameter dependence enters only in the Born term in (3.19). The explanation of this fact is very simple if we recall that the logarithmic contribution originates from the integration over transverse momenta with large $q^2/4$ where q^2 is the momentum transferred along the DGLAP ladder. Therefore, we have two choices:

(i) $t > Q_2^2$ and in this case all logs can be summed in a function with the argument $\ln(Q_1^2/q^2)$,

(ii) $t < Q_2^2$ and in this case we have a function of $\ln(Q_1^2/Q_2^2)$ as in (3.20). In our problem we are certainly dealing with the second case since we are mostly interested in the large b_t behaviour of the scattering amplitude which corresponds to a low q^2 behaviour.

3.2 Many parton showers interactions

Since the colour dipoles are correct degrees of freedom the unitarity constraints are for the dipole–dipole elastic amplitude $a_{\text{el}}(x, r_{1,t}, r_{2,t}; b_t)$ are diagonal and they have the form

$$\begin{aligned} 2 \text{Im} a_{\text{el}}(x, r_{1,t}, r_{2,t}; b_t) & \\ \equiv \sigma(x, r_{1,t}, r_{2,t}; b_t) & \\ = |a_{\text{el}}(x, r_{1,t}, r_{2,t}; b_t)|^2 + G_{\text{in}}(x, r_{1,t}, r_{2,t}; b_t), & \end{aligned} \quad (3.24)$$

where G_{in} stands for the contribution of all inelastic processes. Equation (3.24) is exact for dipole–dipole scattering while it has only a limited accuracy, for example, for dipole–proton scattering [11]. An experimental manifestation of the poor accuracy of (3.24) for deep inelastic scattering is the large cross section of the so-called inelastic diffraction dissociation of proton in an excited state.

Assuming that at high energies the amplitude is pure imaginary, one can find a simple solution to (3.24), namely,

$$a_{\text{el}}(x, r_{1,t}, r_{2,t}; b_t) = i \left(1 - e^{-\frac{\Omega(x, r_{1,t}, r_{2,t}; b_t)}{2}} \right); \quad (3.25)$$

$$G_{\text{in}}(x, r_{1,t}, r_{2,t}; b_t) = \left(1 - e^{-\Omega(x, r_{1,t}, r_{2,t}; b_t)} \right), \quad (3.26)$$

where Ω is the arbitrary real function.

In the Glauber–Mueller approach the opacity Ω is chosen as

$$\begin{aligned} \Omega(x, r_{1,t}, r_{2,t}; b_t) & \\ = \sigma_{\text{dipole}}^{\text{OPS}}(x, r_{1,t}, r_{2,t}; b_t) & \\ = \sigma_{\text{dipole}}^{\text{BA}}(x, r_{1,t}, r_{2,t}; b_t) xG(x, r_{1,t}^2, r_{2,t}^2), & \end{aligned} \quad (3.27)$$

where $\sigma_{\text{dipole}}^{\text{OPS}}$ is the dipole–dipole cross section in the one parton shower approximation (see Fig. 3). One can guess that the physical interpretation of the Glauber–Mueller formula is simple, namely, it takes into account many parton shower interactions in dipole–dipole scattering, but it does not include the possibility for the partons produced from different parton showers to interact. These interactions lead to a more complicated non-linear evolution equation [17–19, 38]. The influence of non-linear evolution on the photon–photon scattering will be discussed in a separate publication; here we restrict ourselves to the consideration of only the first step of this non-linear evolution, which is the Glauber–Mueller approach.

4 Unitarity bound

Using the Glauber–Mueller formula of (3.25) we can give the unitarity bound for dipole–dipole scattering as well as for the $\gamma^*-\gamma^*$ total cross section (see (1.1)). We consider the Glauber–Mueller formula for the total dipole–dipole cross section, namely,

$$\sigma_{\text{tot}}^{dd} = 2 \int d^2 b_t \left(1 - e^{-\frac{\Omega(x, r_{1,t}, r_{2,t}; b_t)}{2}} \right), \quad (4.28)$$

where the opacity Ω is given in (3.27).

The main idea [28] is to replace the full integration over the impact parameter in the expression for the total cross section, by integration in two different regions:

- (i) the first region is $0 \leq b_t \leq b_0(x)$, and
- (ii) the second one is $b_0 \leq b_t \leq \infty$. In the first region we consider $\Omega/2 > 1$ and replace $\text{Im } a_{e1}$ by 1. On the other hand, in the second region we assume that $\Omega/2 < 1$ and expand (3.25) with respect to Ω , restricting ourselves to the first term of this expansion.

Therefore,

$$\sigma_{\text{tot}}^{dd} < 2\pi \left(\int_0^{b_0^2} db_t^2 1 + \int_{b_0^2}^{\infty} db_t^2 \frac{\Omega}{2} \right). \quad (4.29)$$

4.1 Case $b_0 \ll \frac{1}{2m_\pi}$

Let us assume that $b_0 \ll 1/2m_\pi$. In this case we can use (2.9) (or (2.10)) for the b_t -dependence for both intervals. Taking the integral of (4.29) we have

$$\sigma_{\text{tot}}^{dd} < 2\pi \left(b_0^2(x) + \frac{C(r_{1,t}, r_{2,t}) x G(x, r_{1,t}^2, r_{2,t}^2)}{2(b_0^2(x) + a^2)} \right). \quad (4.30)$$

We follow Froissart's idea which is to evaluate the value of the characteristic impact parameter b_0 , namely, the value of $b_0(x)$ can be found from the following equation:

$$\frac{\Omega(x, r_{1,t}, r_{2,t}; b_0(x))}{2} = 1. \quad (4.31)$$

Indeed, for $b_t > b_0$, $\Omega/2 < 1$, the full formula gives less than the first term of the expansion, while for $b_t < b_0$, $\Omega/2 > 1$, the elastic amplitude for the fixed value of the impact parameter is less than 1. Using (3.19) we obtain the solution of (4.31) in the form

$$\begin{aligned} b_0^2 &= -r_{2,t}^2 (z_2 \bar{z}_2) \\ &+ \frac{\alpha_S}{N_c} \sqrt{\frac{\pi(N_c^2 - 1)}{2}} r_{1,t} r_{2,t} \\ &\times \sqrt{I_0 \left(2 \sqrt{\xi(r_{1,t}, r_{1,t}) \ln(1/x)} \right)}; \end{aligned} \quad (4.32)$$

see (3.20) for the notation.

One can see that (4.32) leads to $b_0^2 \rightarrow e^{\sqrt{\xi(r_{1,t}, r_{1,t}) \ln(1/x)}}$ at $x \rightarrow 0$, which means that $b_0(x)$ increases faster than any power of $\ln(1/x)$.

One can see that b_0^2 becomes negative at rather large values of x . It reflects the fact that (4.31) does not have a solution at all values of x . In other words, $\Omega/2 < 1$ even at $b_t = 0$ for low energies. However, it should be stressed that (4.31) does have a solution at high energies which we are actually dealing with in this paper.

Substituting (4.32) into (4.29) we obtain

$$\sigma_{\text{tot}}^{dd} < 2\pi \left(2b_0^2(x) + r_{2,t}^2 (z_2 \bar{z}_2) \right) \quad (4.33)$$

with b_0 of (4.32). Equation (4.32) is in striking contradiction with the Froissart theorem which states that $\sigma_{\text{tot}}^{dd} \ll \ln^2(1/x)$ (see [33] for more details on the Froissart theorem for the photon interaction).

4.2 Case $b_0 \gg \frac{1}{2m_\pi}$

In this case for $b_t > b_0 > \frac{1}{2m_\pi}$ the integral over κ in (2.15) is concentrated at $\kappa \rightarrow 2m_\pi$ with $\kappa - 2m_\pi \approx 1/b_t$. Since $2m_\pi a \ll 1$ we expand the J_1 function, namely $J_1(\kappa a) = \frac{1}{2} \kappa a$. Since we are interested only in the large b_t behaviour of the opacity Ω ($b_0 \gg \frac{1}{2m_\pi}$) we replace κ^2 under the integral by $(2m_\pi)^2$. The use of the asymptotic behaviour of McDonald's function as well as the simplification, mentioned above, leads to the overall accuracy $1/b_t$ in the pre-exponential factor, which is enough to obtain the unitarity bound. It is worthwhile mentioning that in our numerical calculation the integral of (2.15) was computed without any approximation.

Finally we have the following estimate² for the integral of (2.15)

$$\sigma_{\text{dipole}}^{\text{BA}} \quad (4.34)$$

$$\begin{aligned} &= \pi \alpha_S^2 \frac{N_c^2 - 1}{4N_c^2} (r_{1,t}^2 r_{2,t}^2) (2m_\pi)^2 \int_{2m_\pi}^{\infty} \kappa d\kappa K_0(\kappa b_t) \\ &= \pi \alpha_S^2 \frac{N_c^2 - 1}{4N_c^2} (r_{1,t}^2 r_{2,t}^2) (2m_\pi)^3 \frac{1}{b_t} K_1(2m_\pi b_t) \end{aligned} \quad (4.35)$$

$$\begin{aligned} &\rightarrow \pi \alpha_S^2 \frac{N_c^2 - 1}{4N_c^2} (r_{1,t}^2 r_{2,t}^2) (2m_\pi)^3 \\ &\times \sqrt{\frac{\pi}{4m_\pi b_t^3}} e^{-2m_\pi b_t}, \end{aligned} \quad (4.36)$$

where (4.36) gives the asymptotic behaviour at large b_t ($b_t \gg 1/(2m_\pi)$). Namely, this is the expression we will use for the estimates of the value of b_0 in this case. Substituting (4.36) into (2.15) and (3.27) we find the solution to (4.31), namely

$$\begin{aligned} b_0^{\text{exp}}(x) &= \frac{1}{2m_\pi} \ln \left(\pi \alpha_S^2 \frac{N_c^2 - 1}{4N_c^2} (r_{1,t}^2 r_{2,t}^2) (2m_\pi)^3 \right. \\ &\left. \times \sqrt{\frac{\pi}{4m_\pi b_0^{\text{exp}}(x)^3}} x G(x, r_{1,t}^2, r_{2,t}^2) \right); \end{aligned} \quad (4.37)$$

(4.37) is still an equation for b_0^{exp} which has the asymptotic solution at low x :

$$\begin{aligned} b_0^{\text{exp}}(x) &= \frac{1}{2m_\pi} \ln \left(\pi \alpha_S^2 \frac{N_c^2 - 1}{4N_c^2} (r_{1,t}^2 r_{2,t}^2) (2m_\pi)^4 \right. \\ &\left. \times \sqrt{\frac{\pi}{2}} x G(x, r_{1,t}^2, r_{2,t}^2) \right). \end{aligned} \quad (4.38)$$

² The integral is $\int_{2m_\pi}^{\infty} z K_0(z) dz = K_1(2m_\pi)$. This follows directly from the differential equation for K_0 , namely $\frac{d}{dz}(z K_0(z)) = -z K_0(z)$ which should be integrated over z . Recalling that $-\frac{d}{dz} K_0(z) = K_1(z)$ we obtain the above integral. The alternative way is to use a combination of 6.561(8) and 6.561(16) from [39]

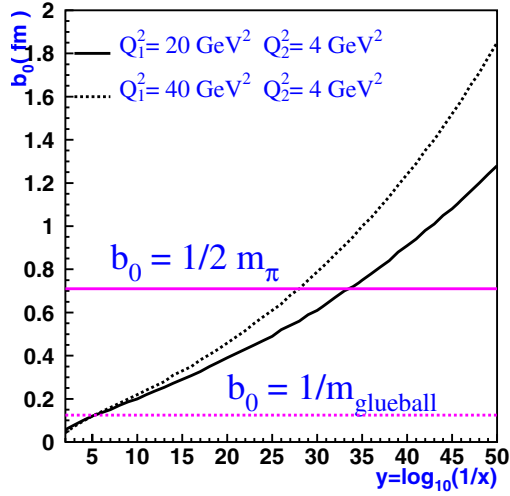


Fig. 4. Energy behaviour of $b_0(x)$ ($Q^2 = 4/r_t^2$)

One can see two important differences between this case and the case that we have considered previously:

- (1) b_0 of (4.38) grows only logarithmically as a function of energy. From (3.20) we conclude that $b_0^{\text{exp}} \propto \sqrt{\ln(1/x)}$;
- (2) the second term in (4.29) gives a small contribution which does not depend on energy.

Therefore, in this kinematic region the unitarity bound has the form

$$\sigma_{\text{tot}}^{\text{dipole-dipole}} < 2\pi (b_0^{\text{exp}}(x))^2, \quad (4.39)$$

with b_0^{exp} from (4.38).

This equation reproduces the classical Froissart result [28], namely, the fact that the total cross section can increase only logarithmically. This is the kind of energy behaviour we expect for DIS or hadron-hadron collisions. However, we would like to draw attention to the fact that we obtain

$$\sigma_{\text{tot}}^{\text{dipole-dipole}} \leq \frac{2\pi}{(2m_\pi)^2} \ln(1/x); \quad (4.40)$$

while the unitarity bound for the hadron-hadron cross section has $\ln^2 s$ behaviour ($\sigma_{\text{tot}}^{\text{hadron-hadron}} \leq \frac{2\pi}{(2m_\pi)^2} \ln^2 s$).

It is worthwhile mentioning that (4.40) holds in the wide range of the photon virtualities which we will define below.

4.3. Predictions

Comparing (4.33) and (4.39), one can see that in a wide range of energies where $b_0(x) \leq 1/2 m_\pi$ the photon-photon scattering shows an exponential ($\propto e^{\sqrt{a \ln(1/x)}}$) behaviour as a function of $\ln(1/x)$, in striking contradiction with the DIS and/or hadronic processes. However, for higher energies $b_0^{\text{exp}}(x)$ reaches the value of $1/2 m_\pi$ or $1/m_{\text{glueball}}$. For higher energies the unitarity bound becomes the one of (4.39). The numerical evaluation shown in Fig. 4 illustrates the fact that the kinematic region of an

exponential increase is wide, especially if we believe that the non-perturbative corrections will only appear at small masses in the t -channel. Therefore, we find that $\gamma^*-\gamma^*$ scattering shows a quite different behaviour than DIS and hadronic processes at all accessible energies (see Fig. 4). However, if the typical mass in the t -channel is rather the mass of a glueball [42] the non-perturbative corrections will stop the exponential increase as $e^{\sqrt{a \ln(1/x)}}$ at $x \approx 10^{-5}$.

It is interesting to notice that the value of $b_0(x)$ turns out to be larger at a larger value of Q^2 in the region of low x . The reason for such a behaviour is the fast increase of the gluon density at larger values of Q^2 , which prevails the suppression due to the extra factor $1/Q$ in (4.32). From Fig. 4 one can see that $b_0(Q^2 = 20 \text{ GeV}^2) < b_0(Q^2 = 40 \text{ GeV}^2)$ at $x \leq 10^{-7}$.

5 Total $\gamma^*-\gamma^*$ for accessible energies

Using the master formula of (1.1) with the dipole-dipole cross section given by (4.28) we calculate the $\gamma^*-\gamma^*$ total cross sections at the accessible range of energies. The results of the calculations are presented in Fig. 5. We fix the virtuality of one of the photons at $Q_2^2 = 4 \text{ GeV}^2$ and calculate the cross section at different values of Q_1^2 . It is essential to recall that we discuss $\gamma^*-\gamma^*$ scattering in the DGLAP dynamics and we have to fix large values for the virtualities of both photons. $Q_2^2 = 4 \text{ GeV}^2$ corresponds to $r_{2,t} \approx 0.2 \text{ fm}$, which is smaller than the electromagnetic radius of the pion ($R_\pi = 0.66 \text{ fm}$). Therefore, we can apply perturbative QCD to our process.

In Fig. 7 we also show the experimental data for the $\gamma^*-\gamma$ process since there is no experimental information about the values of the cross sections for $\gamma^*-\gamma^*$ scattering for large but different photon virtualities. However, the main dependence of the cross section is on the largest virtualities and we can hope that the data on the $\gamma^*-\gamma$ reaction is not very different from the $\gamma^*-\gamma^*$ one.

One can see from Fig. 7 that our predictions are not in contradiction with the available but poor experimental data. We see in Fig. 7 that data with one real photon overshoot our predictions. Actually, there are more data on the $\gamma^*-\gamma$ reaction, but they are presented in the form of the photon structure function. We do not want to recalculate the cross section using these data since we, being theorists, are not entitled to put experimental errors for these reconstructed data. We would like to mention once more that this comparison with experiment could be considered only as an illustrative one showing that we obtain a reasonable estimate for the value of the cross sections. The fact that the data with large but equal virtualities are less than our prediction is understandable, since in our approach the cross sections for such processes do not have an extra enhancement due to the gluon structure function.

Therefore, we can view Fig. 7 as an argument that our predictions do not contradict the current experimental data and as the reason for our expectations that future

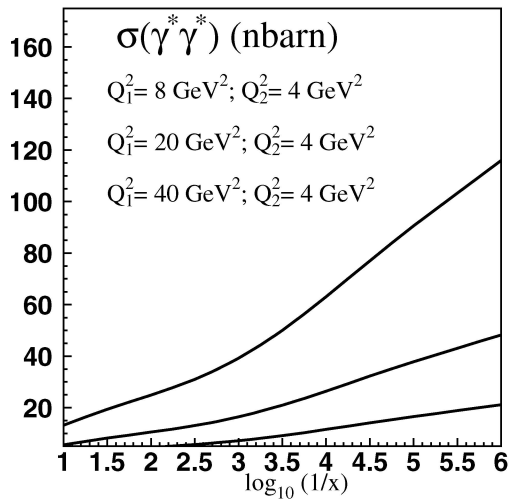


Fig. 5. Energy behaviour of the total $\gamma^*-\gamma^*$ cross section

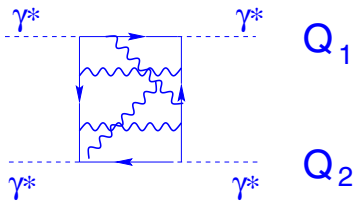


Fig. 6. The picture of the interaction of two photons with virtualities Q_1 and Q_2 due to quark–antiquark pair exchange (the so-called “box” diagram)

experiments will provide us with data which we will be able to compare with our predictions.

It should be mentioned that for serious comparison with the experimental data we have to calculate the power-like corrections to the high energy behaviour discussed in this paper. These corrections are calculable for $\gamma^*-\gamma^*$ scattering and they can be described as the exchange of a quark–antiquark pair in the t -channel (the so-called “box” diagram of Fig. 6) [41]. The simple “box” diagram without gluon emission falls as $1/W^2$, where W is the energy of the $\gamma^*-\gamma^*$ scattering. However, gluon emission slows down this decrease and, therefore, such corrections could be important at sufficiently high energies.

It is instructive also to compare the realistic calculation with the unitarity bound (see Fig. 8). To calculate the unitarity bound we use (1.1) where we substitute

$$\int d^2 b_t \sigma_{a,b}^{dd}(x, r_{1,t}^2, r_{2,t}^2; b_t) = 2\pi (2b_0^2(x) + r_{2,t}^2(z_2 \bar{z}_2)). \quad (5.41)$$

One can see that the unitarity bound considerably overestimates the value of the cross section.

6 Summary

We can summarize our approach in the following way. The kinematic region which we study in this paper is the high

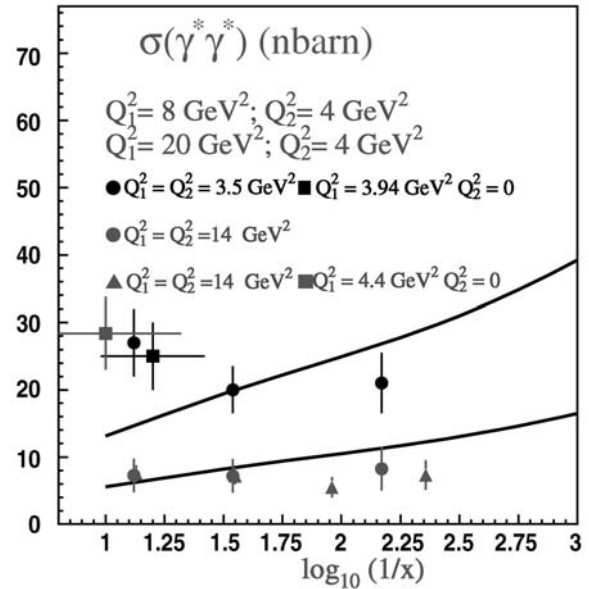


Fig. 7. Energy behaviour of the total $\gamma^*-\gamma^*$ cross section for low energies and experimental data. Squares denote the L3 data [35], while the triangles mark the OPAL data [36]. Circles label data taken from [37]

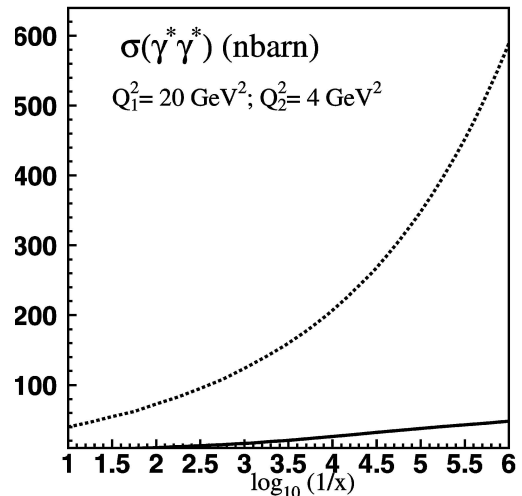


Fig. 8. Energy behaviour of the total $\gamma^*-\gamma^*$ cross section (solid line) and unitarity bound (dotted line)

density QCD region. In this region we have the system of partons at short distances at which α_S is small, but the density of partons has become so large that we cannot apply the usual methods of pQCD. An important method to deal with hdQCD is the Glauber–Mueller approach, which gives the simplest approximation for the high parton density effects. Developing the Glauber–Mueller approach, we obtained the following results.

(1) Both DGLAP and BFKL equations are linear evolution equations predicting a steep growth of the cross sections as a function of energy. However, it is believed that unitarity holds for all physical processes. At high energies it manifests itself as a suppression of the growth of the cross section. At the saturation scale $Q_s(x)$ non-linear ef-

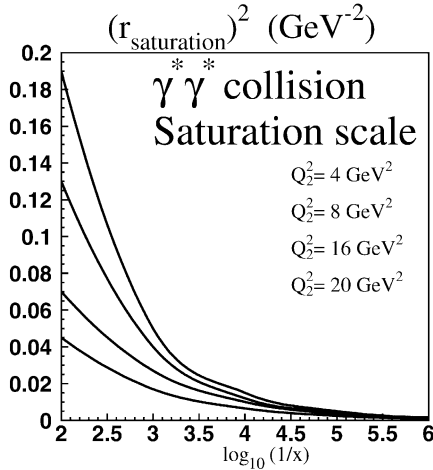


Fig. 9. Estimate of the saturation radius where the transition occurs from low density to high parton density regime. Solution given as dependence of $r_{\text{saturation}}^2$ on $\log_{10}(1/x)$ for fixed values of Q_s^2

fects set in. These effects are due to formation of a high density parton system.

(2) In this paper for the first time the Glauber–Mueller approach has been developed for the case of virtual photon–photon scattering. This allows us to estimate the saturation scale where the transition occurs from the low density to the high parton density regime. The estimate is made from the equation ($r_1 > r_2$)

$$\Omega(b=0, r_{1,\text{saturation}}, r_2)/2 = 1. \quad (6.42)$$

The solution of this equation is shown in Fig. 9.

The solution to (6.42) is proportional to $r_{1,\text{saturation}}^2 \propto r_{2,t}^2 (xG(x, r_{1,\text{saturation}}^2, r_{2,t}^2))^{-1}$.

It is not surprising that the value of $r_{1,\text{saturation}}$ decreases as a function of Q_2 as one can see in Fig. 9. At first sight it looks strange that the value of the saturation scale $Q_s^2 = 4/r_{\text{saturation}}^2$ is rather large. Indeed, for $x = 10^3$ and $Q_2^2 = 4 \text{ GeV}^2$ the value of $Q_s^2 \approx 70 \text{ GeV}^2$ is much larger than expected, $Q_s^2 \approx 1\text{--}2 \text{ GeV}^2$ for the proton.

To understand this difference we take the parameterization of the gluon structure function for the proton in the form of (3.20), namely $xG(x, Q^2) = G_0 I_0(2\sqrt{\xi(2/Q, R_p)} \ln(1/x))$ [40]. R_p is the proton radius which in this estimate we can take $R^2 = 10 \text{ GeV}^{-2}$. G_0 is equal 0.136. One can obtain

$$\frac{Q_s^2(\gamma^* - \gamma^*)}{Q_s^2(\gamma^* - \text{proton})} \propto Q_2^2 R_p^2 (1/G_0) \approx 70.$$

Therefore, we claim that the large value of the saturation momentum is one of the interesting features of the $\gamma^*-\gamma^*$ scattering at high energy.

(3) We note that the gluon interaction leads to a power-like decrease of the opacity (Ω) in Glauber–Mueller formula as a function of the impact parameter (b), namely

$\Omega \propto 1/b_t^4$. It turns out that because of this behaviour the $\gamma^*-\gamma^*$ cross section has a wide range of energy where it increases faster than any power of $\ln(1/x)$, in remarkable contradiction with hadron–hadron and deep inelastic cross sections, which can have only $\ln^2 W$ growth with energy [28]. This fast increase of the $\gamma^*-\gamma^*$ cross section continues up to energies at which the typical impact parameter ($b_0(x)$) will reach the value of $1/2 m_\pi$ ($b_0 = 1/2 m_\pi$; see Fig. 4).

(4) The influence of this power-like b_t behaviour on the unitarity bound is studied. This bound is calculated to give an estimate for the energy behaviour of the cross section.

(5) It is shown that non-perturbative contributions are needed even for the case of photon–photon scattering with large virtualities of both photons in order to describe the large b_t behaviour of the dipole–dipole scattering amplitude.

(6) We found that the unitarity bound for the dipole–dipole cross section for very high energies is $\sigma(\gamma^*-\gamma^*) \leq \frac{2\pi}{(2m_\pi)^2} \ln(1/x)$. This result can be translated in the unitarity bound for the $\gamma^*-\gamma^*$ cross section after integration over $r_{1,t}$ and $r_{2,t}$ in (1.1).

For $Q_2^2 \ll Q_1^2 \leq Q_{1,\text{sat}}^2 = 4/r_{1,\text{saturation}}^2$ we obtain

$$\begin{aligned} \sigma_{T,T}(\gamma^* - \gamma^*) &\leq \sum_{a,b} \left(\frac{4\alpha_{\text{em}}}{\pi} \right)^2 Z_a^2 Z_b^2 \\ &\times \ln(Q_{1,\text{sat}}^2/Q_1^2) \ln(Q_{1,\text{sat}}^2/Q_2^2) \left(\frac{2\pi}{(2m_\pi)^2} \right) \ln(1/x); \\ \sigma_{T,L}(\gamma^* - \gamma^*) &\leq \sum_{a,b} \left(\frac{4\alpha_{\text{em}}}{\pi} \right) \left(\frac{6\alpha_{\text{em}}}{\pi} \right) Z_a^2 Z_b^2 \\ &\times \ln(Q_{1,\text{sat}}^2/Q_1^2) \left(\frac{2\pi}{(2m_\pi)^2} \right) \ln(1/x); \\ \sigma_{L,T}(\gamma^* - \gamma^*) &\leq \sum_{a,b} \left(\frac{4\alpha_{\text{em}}}{\pi} \right) \left(\frac{6\alpha_{\text{em}}}{\pi} \right) Z_a^2 Z_b^2 \\ &\times \ln(Q_{1,\text{sat}}^2/Q_2^2) \left(\frac{2\pi}{(2m_\pi)^2} \right) \ln(1/x); \\ \sigma_{L,L}(\gamma^* - \gamma^*) &\leq \sum_{a,b} \left(\frac{6\alpha_{\text{em}}}{\pi} \right)^2 Z_a^2 Z_b^2 \\ &\times \left(\frac{2\pi}{(2m_\pi)^2} \right) \ln(1/x). \end{aligned} \quad (6.43)$$

In (6.43) for the transverse polarized photon we used the logarithmic approximation in the integral over r_t . Indeed, $|\Psi_T|^2 \propto 1/r_t^2$ and it should be integrated from $4/Q_{\text{sat}}^2$ to $4/Q^2$. Taking into account that $Q_{\text{sat}}^2 \propto xG \propto e^2 \sqrt{\xi(r_{1,t}, r_{2,t}) \ln(1/x)}$ (see (3.21)) one can see that

$$\sigma_{T,T}(\gamma^* - \gamma^*) \leq \frac{C_{T,T}}{(2m_\pi)^2} \ln^2(1/x); \quad (6.44)$$

$$\sigma_{T,L}(\gamma^* - \gamma^*) \leq \frac{C_{T,L}}{(2m_\pi)^2} \ln^{\frac{3}{2}}(1/x); \quad (6.45)$$

$$\sigma_{L,L}(\gamma^* - \gamma^*) \leq \frac{C_{L,L}}{(2m_\pi)^2} \ln^2(1/x). \quad (6.46)$$

Therefore, only $\sigma_{T,T}$ has the same energy dependence of the unitarity bound as the hadron–hadron cross section.

(7) Our approach shows that the non-perturbative corrections at large b_t should be taken into account in the Born cross section. Another way to treat this result is to say that the non-perturbative corrections can be taken into account only in the initial conditions as was discussed in [29,30]. We do not see that such corrections are needed in the kernel of the non-linear evolution equation [38] as was argued in [21–24].

The estimates of at what energies such corrections will enter the game are presented and discussed.

(8) Numerical calculations are performed for the values of the total cross section for accessible energies and virtualities. These predictions will be checked soon with new coming data.

We hope that this paper will stimulate further experimental study of $\gamma^*-\gamma^*$ processes, which can give very conclusive information on the saturation kinematic region in QCD.

Acknowledgements. We would like to thank the DESY Theory Group for their hospitality and for the creative atmosphere during several stages of this work. We wish to thank Jochen Bartels, Errol Gotsman and Uri Maor for very fruitful discussions on the subject. This research was supported in part by the BSF grant # 9800276, by the GIF grant # I-620-22.14/1999 and by the Israeli Science Foundation, founded by the Israeli Academy of Science and Humanities.

References

1. A. De Roeck, Two Photon Physics at Future Linear Colliders, hep-ph/0101075; A.J. Finch, Test of QCD in Two Photons Physics at LEP, hep-ph/0102110 and references therein
2. E.A. Kuraev, L.N. Lipatov, V.S. Fadin, Sov. Phys. JETP **45**, 199 (1977); Ia.Ia. Balitsky, L.N. Lipatov, Sov. J. Nucl. Phys. **28**, 822 (1978); L.N. Lipatov, Sov. Phys. JETP **63**, 904 (1986)
3. J. Bartels, A. De Roeck, H. Lotter, Phys. Lett. B **389**, 742 (1996)
4. S.J. Brodsky, F. Hautmann, D.E. Soper, Phys. Rev. D **56**, 6957 (1997)
5. M. Boonekamp et al., Nucl. Phys. B **555**, 540 (1999)
6. J. Kwiecinski, L. Motyka, Phys. Lett. B **462**, 203 (1999)
7. J. Kwiecinski, L. Motyka, A. De Roeck, The QCD pomeron at TESLA: Motivation and exclusive J/psi production, hep-ph/0001180
8. N.G. Evanson, J.R. Forshaw, Diffractive production of high p(t) photons at a future linear collider, hep-ph/9912487
9. E. Gotsman, E. Levin, U. Maor, E. Naftali, Eur. Phys. J. C **14**, 511 (2000)
10. N. Timneanu, J. Kwiecinski, L. Motyka, Saturation model for two gamma physics, hep-ph/0206130; Eur. Phys. J. C **23**, 513 (2002), hep-ph/0110409
11. A.H. Mueller, Nucl. Phys. B **335**, 115 (1990)
12. E.M. Levin, M.G. Ryskin, Sov. J. Nucl. Phys. **45**, 150 (1987)
13. A. Zamolodchikov, B. Kopeliovich, L. Lapidus, JETP Lett. **33**, 595 (1981)
14. A.H. Mueller, Nucl. Phys. B **415**, 373 (1994)
15. A. Donnachie, H.G. Dosch, M. Rueter, Eur. Phys. J. C **13**, 141 (2000)
16. N.N. Nikolaev, B.G. Zakharov, Z. Phys. C **49**, 607 (1991); E.M. Levin, A.D. Martin, M.G. Ryskin, T. Teubner, Z. Phys. C **74**, 671 (1997)
17. L.V. Gribov, E.M. Levin, M.G. Ryskin, Phys. Rep. **100**, 1 (1983)
18. A.H. Mueller, J. Qiu, Nucl. Phys. B **268**, 427 (1986)
19. L. McLerran, R. Venugopalan, Phys. Rev. D **49**, 2233, 3352 (1994); D **50**, 2225 (1994); D **53**, 458 (1996); D **59**, 09400 (1999)
20. K. Golec-Biernat, M. Wusthoff, Eur. Phys. J. C **20**, 313 (2001); Phys. Rev. D **60**, 114023, 014017 (1999)
21. A. Kovner, U.A. Wiedemann, Taming the BFKL Intercept via Gluon Saturation, hep-ph/0208265
22. A. Kovner, U.A. Wiedemann, No Froissart bound from gluon saturation, hep-ph/0207335
23. A. Kovner, U.A. Wiedemann, Perturbative saturation and the soft pomeron, hep-ph/0204277
24. A. Kovner, U.A. Wiedemann, Nonlinear QCD evolution: Saturation without unitarization, hep-ph/0112140
25. V.N. Gribov, L.N. Lipatov, Sov. J. Nucl. Phys. **15**, 438 (1972); L.N. Lipatov, Yad. Fiz. **20**, 181 (1974); G. Altarelli, G. Parisi, Nucl. Phys. B **126**, 298 (1977); Yu.L. Dokshitzer, Sov. Phys. JETP **46**, 641 (1977)
26. G.P. Lepage, S.J. Brodsky, Phys. Rev. D **22**, 2157 (1980)
27. I.F. Ginzburg, S.L. Panfil, V.G. Serbo, Nucl. Phys. B **284**, 685 (1987); B **296**, 569 (1988); I.F. Ginzburg, D. Yu. Ivanov, Nucl. Phys. B **388**, 376 (1992); D.Y. Ivanov, R. Kirschner, Phys. Rev. D **58**, 114026 (1998), hep-ph/9807324
28. M. Froissart, Phys. Rev. **123**, 1053 (1961); A. Martin, Scattering theory: unitarity, analyticity and crossing, Lecture Notes in Physics (Springer-Verlag, Berlin-Heidelberg-New York 1969)
29. E.M. Levin, M.G. Ryskin, Phys. Rept. **189**, 267 (1990)
30. E. Ferreira, E. Iancu, K. Itakura, L. McLerran, Froissart bound from gluon saturation, hep-ph/0206241
31. P. Colangelo, A. Khodjamirian, QCD sum rules: A modern perspective, hep-ph/0010175; V.E. Markushin, Acta Phys. Polon. B **31**, 2665 (2000); O.I. Yakovlev, R. Ruckl, S. Weinzierl, QCD sum rules for heavy flavors, hep-ph/0007344; M.A. Shifman, QCD Sum Rules, in Lectures on QCD: Foundations, edited by F. Lenz et al., pp. 170–187; S. Narison, QCD Spectral Sum Rules, World Sci. Lect. Notes Phys. **26**, 1 (1989); M.A. Shifman, A.I. Vainshtein, V.I. Zakharov, Nucl. Phys. B **147**, 385, 448, 519 (1979)
32. R.K. Ellis, Z. Kunszt, E.M. Levin, Nucl. Phys. B **420**, 517 (1994) [Erratum B **433**, 498 (1995)]
33. E. Gotsman, E.M. Levin, U. Maor, Eur. Phys. J. C **5**, 303 (1998), hep-ph/9708275
34. E. Gotsman, E. Levin, U. Maor, Nucl. Phys. B **464**, 251 (1996), hep-ph/9509286

35. L3 Collaboration, M. Acciari et al., Phys. Lett. B **453**, 333 (1999); L3 Note 2404
36. F. Wackerle, Nucl. Phys. Proc. Suppl. **71**, 381 (1997), hep-ex/9710005
37. Aihara et al., Phys. Rev. D **41**, 2667 (1990)
38. Ia. Balitsky, Nucl. Phys. B **463**, 99 (1996); Yu. Kovchegov, Phys. Rev. D **60**, 034008 (2000)
39. I. Gragstein, I. Ryzhik, Tables of series, products, and integrals (Verlag MIR, Moskau 1981)
40. A.L. Ayala Filho, M.B. Gay Ducati, E.M. Levin, Eur. Phys. J. C **8**, 11 (1999), hep-ph/9710539
41. B. Ermolaev, R. Kirschner, L. Szymanowski, Eur. Phys. J. C **7**, 65 (1999), hep-ph/9806439; R. Kirschner, L. Mankiewicz, A. Schafer, L. Szymanowski, Z. Phys. C **74**, 501 (1997), hep-ph/9606267; J. Bartels, B.I. Ermolaev, M.G. Ryskin, Z. Phys. C **70**, 273 (1996), hep-ph/9507271; J. Bartels, B.I. Ermolaev, M.G. Ryskin, Z. Phys. C **72**, 627 (1996), hep-ph/9603204; R. Kirschner, L.N. Lipatov, Nucl. Phys. B **213**, 122 (1983)
42. A. Vaccarino, D. Wengarten, Phys. Rev. D **60**, 114501 (1999)